Appl Microbiol Biotechnol (2016) 100:8901–8912
DOI 10.1007/s00253-016-7711-5

APPLIED MICROBIAL AND CELL PHYSIOLOGY

Understanding the physiological roles of polyhydroxybutyrate (PHB) in *Rhodospirillum rubrum* S1 under aerobic chemoheterotrophic conditions

Tanja Narancic[1,2] · Elisa Scollica[1,2] · Shane T. Kenny[3] · Helena Gibbons[4] · Eibhlin Carr[4] · Lorraine Brennan[4] · Gerard Cagney[5] · Kieran Wynne[5] · Cormac Murphy[2] · Matthias Raberg[6] · Daniel Heinrich[6] · Alexander Steinbüchel[6,7] · Kevin E. O'Connor[1,2]

Received: 24 June 2016 / Accepted: 28 June 2016 / Published online: 1 August 2016
© Springer-Verlag Berlin Heidelberg 2016

Abstract Polyhydroxybutyrate (PHB) is an important biopolymer accumulated by bacteria and associated with cell survival and stress response. Here, we make two surprising findings in the PHB-accumulating species *Rhodospirillum rubrum* S1. We first show that the presence of PHB promotes the increased assimilation of acetate preferentially into biomass rather than PHB. When *R. rubrum* is supplied with ^{13}C-acetate as a PHB precursor, 83.5 % of the carbon in PHB comes from acetate. However, only 15 % of the acetate ends up in PHB with the remainder assimilated as bacterial biomass. The PHB-negative mutant of *R. rubrum* assimilates 2-fold less acetate into biomass compared to the wild-type strain. Acetate assimilation proceeds via the ethylmalonyl-CoA pathway with (*R*)-3-hydroxybutyrate as a common intermediate with the PHB pathway. Secondly, we show that *R. rubrum* cells accumulating PHB have reduced ribulose 1,5-bisphosphate carboxylase (RuBisCO) activity. RuBisCO activity reduces 5-fold over a 36-h period after the onset of PHB. In contrast, a PHB-negative mutant maintains the same level of RuBisCO activity over the growth period. Since RuBisCO controls the redox potential in *R. rubrum*, PHB likely replaces RuBisCO in this role. *R. rubrum* is the first bacterium found to express RuBisCO under aerobic chemoheterotrophic conditions.

Keywords *Rhodospirillum rubrum* S1 · Aerobic growth · Polyhydroxybutyrate (PHB) · Ribulose 1,5-bisphosphate carboxylase (RuBisCO) · Crotonyl-CoA carboxylase/reductase · Ethylmalonyl-CoA pathway

Tanja Narancic and Elisa Scollica contributed equally to this work.

Electronic supplementary material The online version of this article (doi:10.1007/s00253-016-7711-5) contains supplementary material, which is available to authorized users.

✉ Kevin E. O'Connor
kevin.oconnor@ucd.ie

1 UCD Earth Institute, O'Brien Centre for Science, University College Dublin, Belfield, Dublin 4, Ireland

2 School of Biomolecular and Biomedical Science, University College Dublin, Belfield, Dublin 4, Ireland

3 NovaUCD, Belfield Innovation Park, University College Dublin, Bioplastech Ltd., Belfield, Dublin 4, Ireland

4 Institute of Food and Health and Conway Institute, University College Dublin, Belfield, Dublin 4, Ireland

5 School of Biomolecular and Biomedical Sciences, Conway, University College Dublin, Belfield, Dublin 4, Ireland

6 Institut für Molekulare Mikrobiologie und Biotechnologie, Westfälische Wilhelms-Universität, Münster, Germany

7 Environmental Sciences Department, King Abdulaziz University, Jeddah, Saudi Arabia

Introduction

Rhodospirillum rubrum has a powerful set of metabolic tools allowing photoautotrophy, chemoautotrophy, photoauto lithotrophy, and heterotrophy (Gordon and McKinlay 2014; Imhoff and Trüper 1992; Munk et al. 2011; Selao et al. 2011). This bacterium is well studied due to its biotechnological potential in the production of pigments, vitamins, coenzymes (Carius et al. 2013), and hydrogen (Basak and Das 2007). *R. rubrum* is also known to accumulate the biopolymer polyhydroxybutyrate (PHB) with the vast majority of PHB accumulation studies performed in anaerobic conditions (Brandl et al. 1989; Do et al. 2007; Smith et al. 2008). PHB is primarily considered a carbon and energy storage polymer, accumulated as a response to a nutrient imbalance conditions

(Steinbüchel and Lütke-Eversloh 2003). There is growing evidence supporting additional physiological roles of this type of biopolymer. A link between polyhydroxyalkanoate (PHA) accumulation and stress tolerance was observed in *P. aeruginosa*, showing that PHA has more roles than merely a carbon and energy storage molecule (Jendrossek and Pfeiffer 2014; Pham et al. 2004; Raberg et al. 2014; Zhao et al. 2007). There are suggestions that PHA metabolism also acts as a regulatory mechanism optimising the carbon and energy flow in the cell (Arias et al. 2013; Eggers and Steinbüchel 2014; Escapa et al. 2012). It has been speculated that PHB has a potential to act as an electron sink during anaerobic photo heterotrophic growth of *R. rubrum* (Gordon and McKinlay 2014).

In the current study, we performed a proteomic analysis of chemoheterotrophic growth of *R. rubrum* under PHB-accumulating conditions, which showed the expression of ribulose 1,5-bisphosphate carboxylase (RuBisCO), the ethylmalonyl-CoA (EMC) pathway and biopolymer PHB accumulation proteins. We undertook biochemical and physiological studies to examine the effect of stimulated PHB accumulation on metabolic processes in *R. rubrum*. We show here that RuBisCO, an enzyme previously exclusively associated with anaerobic and photosynthetic growth (Grammel et al. 2003), is active in *R. rubrum* under aerobic growth conditions in the dark, but the expression and activity are negatively influenced by PHB accumulation. Moreover, PHB unusually stimulates acetate assimilation into biomass and not into further PHB accumulation. Finally, the EMC pathway is used for acetate assimilation in *R. rubrum*, with the level and profile of crotonyl carboxylase/reductase (Ccr) activity similar in the wild type and mutant with a 6-h time delay between them for when maximum Ccr activity is observed.

Materials and methods

Bacterial strain, medium and growth conditions All experiments were performed with *R. rubrum* S1 strain (ATCC 11170) or *R. rubrum* Δ*pha*C1Δ*pha*C2 (Klask et al. 2015). Cultures were grown in modified SMN medium (Bose et al. 1961) containing the following, per litre: 3 g KH_2PO_4; 4.5 g K_2HPO_4; 0.2 g $MgSO_4{\cdot}7H_2O$; 75 mg $CaCl_2{\cdot}2H_2O$; 20 mg EDTA; 0.1 mL vitamin solution (per litre: 150 mg biotin; 44 mg thiamine hydrochloride; 44 mg nicotinamide; 22 mg *p*-aminobenzoic acid; 22 mg riboflavin); 1 mL trace elements solution (per litre: 4 g $ZnSO_4{\cdot}7H_2O$; 1 g $MnCl{\cdot}4H_2O$; 0.2 g $Na_2B_4O_7{\cdot}10H_2O$; 0.3 g $NiCl_2{\cdot}6H_2O$; 1 g $Na_2MoO_4{\cdot}2H_2O$; 1 g $CuCl{\cdot}2H_2O$; 7.6 g $FeSO_4{\cdot}7H_2O$) and 1.25 g for full or 0.31 g $(NH_4)_2SO_4$ for nitrogen-limited growth.

Precultures of *R. rubrum* were incubated for 48 h in 2 mL of modified SMN medium in 13-mL sterile Sarstedt tubes wrapped in tin foil at 30 °C and 200 rpm in the dark. *R. rubrum* cultures were grown in 250-mL conical flasks wrapped in aluminium foil, containing 50 mL of modified SMN medium, at 30 °C and 200 rpm in the dark. For cultures grown with malate and acetate (MA) 4 g L^{-1} disodium malate (Sigma-Aldrich, Dublin, Ireland) and 3.7 g L^{-1} sodium acetate (Sigma-Aldrich, Dublin, Ireland) were added. These quantities corresponded to an equal amount of carbon (1.08 g_c L^{-1}) coming from each carbon source. Acetate was added at T24. For control experiments, *R. rubrum* was grown with 8 g L^{-1} (2.16 g_C L^{-1}) disodium malate (M) as a sole source of carbon and energy.

Cell density and photosynthetic membrane formation was monitored spectrophotometrically (OD_{660}, OD_{680}, OD_{880}; Unicam Helios d UV/VIS spectrophotometer). Cell dry weight (CDW) was obtained by lyophilising the cell pellet (FreeZone Plus 6 Liter Cascade Freeze Dry Systems, Labconco, Missouri, USA) obtained after centrifugation. The photosynthetic membrane formation was assessed using OD_{880}/OD_{660} ratio (Carius et al. 2011), which was in the range 0.5–0.55 in all our experiments indicating that the cultures were fully aerobic.

Cells were collected at different time points of growth for different experiments, harvested by centrifugation (5000 *g* for 10 min at 4 °C; Benchtop 5430R centrifuge; Eppendorf, Hamburg, Germany) and washed twice with 10 mL of phosphate buffer (50 mM, pH 7). The pellets were used immediately for further analysis or stored at −80 °C.

PHA extraction and content determination The polymer content was assayed by subjecting the lyophilised cells to acidic methanolysis as previously described (Lageveen et al. 1988). The PHA monomers' methylesters were assayed by GC using a Hewlett-Packard 6890N chromatograph equipped with an HP-Innowax capillary column (30 m × 0.25 mm, 0.50 μm film thickness; Agilent Technologies) and a flame ionisation detector (FID), using the temperature programme previously described (Lageveen et al. 1988). Total PHA content was determined as a percentage of CDW.

Nutrient analysis Nitrogen concentration (absolute amount of N) was determined using the method of Scheiner (1976). Malate utilisation was determined from supernatant by HPLC using a C18 ACE column (250 mm × 4.6 mm, particle size 5 μm; Advanced Chromatographic Technologies Ltd.). The samples were isocratically eluted with 20 mM KH_2PO_4 (pH 2)/methanol (95:5) at a flow rate of 1 mL min^{-1}. Acetate consumption was determined by acidifying 1 mL of the supernatant with 50 % H_2SO_4 (*v*/*v*), followed by addition of 100 μL saturated NaCl and extraction with 3 mL of chloroform/methanol (1:1, *v*/*v*) solution. The

organic layer was analysed by a GC-FID detector fitted with an HP-Innowax column (30 m × 0.25 mm, 0.25 μm film thickness, Agilent Technologies), using the following conditions: 120 °C for 1 min, temperature ramp for 10 °C min^{-1} up to 250 °C and holding for 2 min.

Protein concentration The protein concentration was measured using the Bicinchoninic Acid Kit (Sigma-Aldrich, Dublin, Ireland).

Proteomic analysis Pellets obtained from 50-mL cultures grown with M or MA for 24, 30 or 72 h were lysed in an appropriate volume of 8 M urea solution to give a uniform protein concentration of 100 μg μL^{-1}. The samples were reduced with 5 mM dithiothreitol and alkylated with 10 mM iodoacetamide. pH was adjusted to 7 with 200 mM NH_4HCO_3, and proteins were digested using proteomics grade trypsin in a convenient, single-use 1-μg package (Trypsin Singles, Sigma-Aldrich, Dublin, Ireland). The pH of the solution was brought to 2.5 with formic acid, and peptides were purified using ZipTip C18 columns (Merck Millipore, Cork, Ireland). The resulting tryptic peptide mixtures were resuspended in 0.1 % (*v*/*v*) formic acid and analysed by Q Exactive Hybrid Quadropole-Orbitrap Mass Spectrometer (MS) (Thermo Scientific, Paisley, UK) connected to a Dionex UltiMate 3000 (RSLCnano) chromatography system (buffer A: 97 % water, 2.5 % acetonitrile, 0.5 % acetic acid; buffer B: 97 % acetonitrile, 2.5 % water, 0.5 % acetic acid. All solvents are of LCMS grade). Each sample was loaded onto a fused silica emitter (75 μm ID, pulled using a laser puller (Sutter Instrument P2000)), packed with Reprocil Pur C18 (1.9 μm) reverse phase media column, and was separated by an increasing acetonitrile gradient over 60 min at a flow rate of 250 nL min^{-1}. The mass spectrometer was operated in positive ion mode with a capillary temperature of 320 °C and a potential of 2300 V applied to the frit. All data was acquired with the MS operating in automatic data-dependent switching mode. A high-resolution (70,000) MS scan (300–1600 m/z) was performed using the Q Exactive to select the 12 most intense ions prior to MS/MS analysis using HCD.

Spectra were identified, and proteins were quantified using the Andromeda peptide identification algorithm integrated into MaxQuant (Cox and Mann 2008; Cox et al. 2011), searching against the UniProt database of *R. rubrum* S1 (www.uniprot.org, downloaded October 23, 2013). Proteins with a 1.5-fold change or higher and a significant change in *t* test (FDR 0.05; S0 0.1) were automatically accepted, while spectra with no specific change were manually checked for quality. Label-free quantification (LFQ) was used to compare the expression level of proteins present in different samples (Wang et al. 2003). David bioinformatics was used for the functional annotation and addition of KEGG pathways (KEGG 2015; Huang Da et al. 2009).

Metabolomic analysis The pellets obtained from 50-mL cultures were resuspended in an appropriate volume of cold methanol 75 % (*v*/*v*) with respect to total protein concentration (80 μg μL^{-1}). Cell suspensions were sonicated for 10 min on ice (Sonic Dismembrator FB120, Fisher Scientific, Dublin, Ireland; 40 % amplitude, 1 s on 1 s off) and centrifuged for 5 min (16,000 *g*, 4 °C), and the cell extracts were dried under a flush of N_2. Samples were reconstituted with 590 μL deuterium oxide and 10 μL sodium trimethyl-[2,2,3,3-^{2}H4]-propionate (TSP) (0.005 g mL^{-1}). ^{1}H nuclear magnetic resonance (NMR) spectra were acquired on a 600-MHz Varian NMR spectrometer (Varian Limited, Oxford, UK) by using the first increment of a nuclear Overhauser effect spectroscopy (NOESY) pulse sequence at 25 °C. Spectra were acquired with 16,384 data points and 512 scans. Water suppression was achieved during the relaxation delay (2.5 s) and the mixing time (100 ms). All spectra were referenced to TSP at 0.0 ppm. ^{1}H NMR spectra were processed manually with Chenomx software (version 7.5; Chenomx Edmonton, Canada) and were phase and baseline corrected. The metabolites were quantified using Chenomx Profiler. Statistical analyses were performed using IBM SPSS Statistics 20. Differences in metabolic levels across the sample groups were examined using ANOVA and independent *t* tests.

Enzymatic assays Harvested cells were resuspended in phosphate buffer (50 mM, pH 7), lysed using BugBuster (Merck Millipore) according to the manufacturer's instructions and centrifuged (16,000 *g*, 30 min, 4 °C). The supernatant was used for the assays. The total protein concentration in the supernatant was determined by BCA assay. All enzymatic assays were performed in triplicate for each time point, and results were statistically analysed using ANOVA and independent *t* tests.

Ribulose 1,5-biphosphate carboxylase activity assay The activity of RuBisCO was determined by following the rate of NADH (Sigma; ε_{NADH} = 6.3 mM^{-1} cm^{-1}) oxidation by cell-free extracts of *R. rubrum* at 340 nm as previously described (Reid et al. 1997). Briefly, the assay (200 μL) contained 100 mM bicine buffer (pH 8), 25 mM $KHCO_3$, 0.25 mM NADH, 3.5 mM ATP, 20 mM $MgCl_2$, 5 mM phosphocreatine, 4.7 U glyceraldehyde-3-phosphate dehydrogenase from rabbit muscle (E.C. 1.2.1.12; Sigma-Aldrich, Dublin, Ireland), 4.7 U 3-phosphoglyceric phosphokinase from baker's yeast (E.C 2.7.2.3; Sigma-Aldrich, Dublin, Ireland), 4.7 U creatine phosphokinase from bovine heart (E.C 2.7.3.2; Sigma-Aldrich, Dublin, Ireland) and 20 μL of cell-free extract containing 100 μg μL^{-1} of total proteins as a source of RuBisCO. The reaction was started by adding 0.5 mM ribulose 1,5-bisphosphate (Sigma-Aldrich, Dublin, Ireland). Appropriate controls were used to demonstrate the specificity of the reaction, including reactions without ribulose

1,5-bisphosphate or NADH, and a reaction with cell-free extract boiled at 100 °C for 5 min (negative controls).

Crotonyl-CoA carboxylase/reductase activity assay The enzymatic activity of Ccr was assayed as previously described (Erb et al. 2009a), with slight modifications. Cell-free extract was used as a source of Ccr activity. The 182-μL standard reaction contained the following: 180 mM Tris–HCl (pH 7.9), 0.25 mM NADH or NADPH (Sigma-Aldrich, Dublin, Ireland), 0.5 mM crotonyl-CoA (Sigma-Aldrich, Dublin, Ireland) and 20 μL of cell-free extract (100 μg/μL total protein concentration). The reaction was started by the addition of mixture of 20 μL 50 mM $KHCO_3$ and 6 μL 1 M acetic acid to dissolve CO_2 from bicarbonate by acidification. This "CO_2 solution" was immediately added to the reaction mixture, and decrease in absorbance was followed at 340 nm (ε_{NADH} = 6.3 mM^{-1} cm^{-1}). Appropriate controls were used to demonstrate the specificity of the reaction, including a reaction without crotonyl-CoA (negative control), a reaction without CO_2 source (crotonyl-CoA reduction reaction), a reaction with cell-free extract boiled at 100 °C for 5 min (negative control) and a reaction without NADH (negative control). The Ccr activity was normalised per total protein concentration.

ATP and NADPH/NADP quantification Intracellular levels of ATP and NADPH/NADP were quantified using a bioluminescent enzymatic kit (ADP/ATP Ratio Assay Kit, Sigma-Aldrich, Dublin, Ireland) and NADPH/NADP quantification kit (Sigma-Aldrich, Dublin, Ireland) according to manufacturers' instructions.

The analysis of the ^{13}C-labelled PHB The strain was grown in 50 mL of SMN, nitrogen limiting, supplemented with disodium malate (non-labelled) and sodium acetate-1-^{13}C added at T24 (Sigma-Aldrich, Dublin, Ireland) for 72 h. The polymer was extracted from lyophilised cells using Soxhlet extraction method (Koller et al. 2005) and hydrolysed. Analysis was conducted using an Agilent 6890 gas chromatograph coupled to a 5973 mass selective detector. The methyl ester of the monomer dissolved in chloroform was injected into an HP5-MS column (30 m × 0.25 mm × 0.25 μm) and oven temperatures held at 60 °C for 4 min, then raised to 170 °C at 10 °C min^{-1} and held at that temperature for 3 min. The mass spectrometer was operated in selected ion monitoring (SIM) mode measuring ion currents *m/z* 103 (corresponding to a monomer molecular ion containing only ^{12}C atoms), 104 (corresponding to a monomer molecular ion containing one ^{13}C and three ^{12}C atoms), 105 (corresponding to a monomer molecular ion containing two ^{13}C and two ^{12}C atoms) and 106 (corresponding to a monomer molecular ion containing three ^{13}C and one ^{12}C atoms). The mass spectrum of the unlabelled and labelled methyl ester, which had a retention time of 3.3 min, is shown in Fig. S1 indicating the key fragment ion *m/z* 103 and 105. Incorporation of isotope enrichment was determined after correcting for natural isotope abundances.

Results

Chemoheterotrophic growth of *R. rubrum* and PHB production

While acetate is a well-known precursor for PHB accumulation, *R. rubrum* cannot utilise acetate aerobically in the dark without the presence of CO_2 or C_4-dicarboxylic acids (Eisenberg 1953). C_4-dicarboxylic acids found in the TCA cycle are good growth substrates for *R. rubrum*, but they are poor substrates for PHB accumulation (Brandl et al. 1989; Ormerod et al. 1961). Thus, we decided to use a combination of MA to allow aerobic growth and sufficient PHB accumulation in *R. rubrum*. We tested acetate addition at different time points (T0, T12, T24; data not shown). Since aerobic metabolism of acetate in the dark requires CO_2 (provided by oxidative decarboxylation of malate to pyruvate and pyruvate to acetyl-CoA), addition of acetate at earlier time points (T0, T12) resulted in lower biomass and PHB yield (data not shown). This is probably due to the known inhibition of the activity of the enzymes of the pyruvate dehydrogenase complex (PDC) by acetyl-CoA (Lüderitz and Klemme 1977). We analysed biomass accumulation, substrate consumption, and PHB accumulation over time when acetate was added to malate grown cultures at T24 (Fig. 1). Acetate assimilation (0.015 g_C L^{-1} h^{-1}) represses malate metabolism, with malate consumption rate decrease from 0.036 to 0.004 g_C L^{-1} h^{-1} observed in the period between T36 and T48 i.e. 12 h after the addition of acetate to cells growing on malate (Fig. 1b). In addition, malate consumption over a 72-h period was 0.009 g_C L^{-1} h^{-1}, while overall malate consumption in the control experiment without acetate addition was 0.017 g_C L^{-1} h^{-1} (Online Resource, Fig. S3). The decrease in malate consumption corresponds to an increased acetate consumption rate and the onset of PHB accumulation (Fig. 1a, b). Besides the 5-fold increase in PHB associated with increased acetate consumption between T36 and T48, there was a 2.5-fold increase in PHB-free biomass (0.24 g L^{-1} at T36 and 0.6 g L^{-1} at T48).

Acetate is a more reduced compound than malate, providing more reducing equivalents. The level of NADPH is an important regulator of PHB metabolism (Hauf et al. 2013); thus, we measured the presence of the oxidised and reduced forms of this molecule in *R. rubrum* S1. An hour after acetate addition, *R. rubrum* cells showed a 2.2-fold higher NADPH/$NADP^+$ ratio in comparison with T24 (Online Resource, Fig. S2A). Acetate addition also coincided with a 1.7-fold increase in ATP levels, (Online Resource, Fig. S2B).

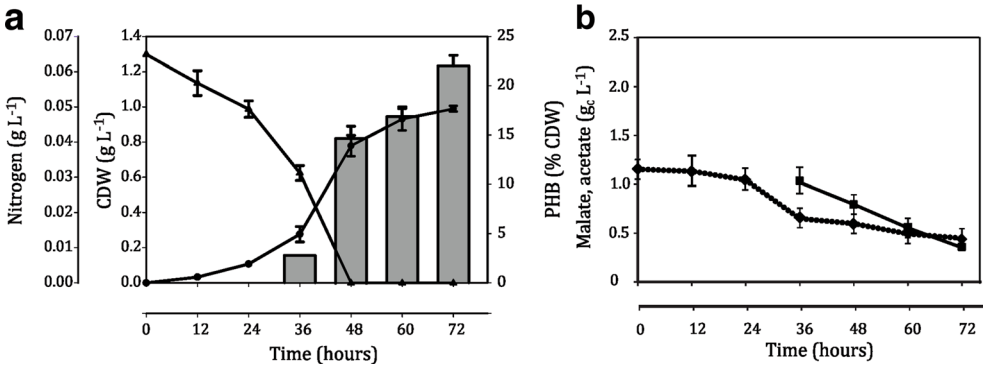

Fig. 1 Growth profile of *R. rubrum* S1 when malate and acetate were used as co-substrates. **a** Cell dry weight, CDW (*filled circle*), nitrogen (*filled triangle*) and PHB accumulation (*grey bars*) when 4 g L^{-1} (1.08 g_C L^{-1}) disodium malate and 3.7 g L^{-1} (1.08 g_C L^{-1}) sodium acetate were used. **b** Malate (*dotted line*, *filled diamond*) and acetate (*full line*, *filled square*) consumption over time. The *error bars* represent standard deviation between three biological replicates

PHB promotes acetate assimilation into biomass

The GC-MS analysis of the PHB polymer extracted at the end of the growth period when ^{13}C-labelled acetate (one carbon atom labelled, ^{13}C-1-acetate) was used showed that 72 % of the PHB monomer units contained two labelled carbons (Table 1; Online Resource, Fig. S1), which means that the monomer unit was formed by condensation of two acetyl-CoA molecules originating from supplied acetate. Twenty-three percent of monomers contained one labelled carbon (Table 1; Online Resource, Fig. S1), suggesting that these monomers are a combination of acetate supplied at T24 (^{13}C-1-acetate) and acetate formed during oxidative decarboxylation of malate to pyruvate followed by oxidative decarboxylation of pyruvate to acetyl-CoA. Thus, acetate accounts for 83.5 % of the monomers in PHB. However, only 15 % of the total acetate consumed was converted into PHB (0.03 g_C L^{-1}). While acetate is a direct precursor to PHB in *R. rubrum*, the conversion is inefficient. We have compared the ability of *R. rubrum* to grow on M and MA. Given that the residual biomass achieved by M- and MA-grown cells was similar and that MA cells showed 2-fold lower malate consumption compared to M-grown cells (Table 1), the remainder of the acetate supplied contributes to biomass generation.

To determine if PHB accumulation affected acetate assimilation into biomass, a double knockout mutant *R. rubrum* Δ*phaC1*Δ*phaC2* (Klask et al. 2015) incapable of PHB accumulation was investigated. The residual biomass achieved by the wild type and the knockout was the same, and the total carbon consumed was the same, but the acetate consumption was 1.9-fold lower in the knockout mutant (Table 1). The PHB-negative mutant consumes 0.38 g_C L^{-1} of acetate (Table 1), while 0.7 g_C L^{-1} of acetate is assimilated into residual (PHB-free) biomass in the wild type. Removing the ability of *R. rubrum* to accumulate PHB reduces its ability to assimilate acetate in biomass.

Proteomic analysis of *R. rubrum* S1

To further the investigation of the metabolism of acetate and PHB accumulation in *R. rubrum*, the proteome of *R. rubrum* was analysed using a "shotgun" approach (Online Resource, Table S1; Table 2). The genome of *R. rubrum* S1 was reported

Table 1 Comparison of growth and PHB accumulation in malate (M)- and malate-acetate (MA)-grown *R. rubrum* S1 and *R. rubrum* Δ*pha*C1Δ*pha*C2, a mutant incapable of PHB accumulation

Strain	Growth substrate	Consumed carbon (g_C L^{-1})	Residual biomass (g L^{-1})	PHB (g L^{-1})	C/PHB yield[b] (%)	Incorporation of ^{13}C (none/single/double)
WT	M	1.27[a]	0.69	0.06	2.4	–
	MA	0.63M + 0.73A	0.76	0.24	9.5	5:23:72
Δ*pha*C1Δ*pha*C2	M	1.36	0.75	0	0	–
	MA	0.82M + 0.38A	0.74	0	0	–

Growth and PHB accumulation were assessed at T72

M malate, *A* acetate

[a] Standard deviation between biological triplicates was <5 %

[b] Carbon to PHB conversion

Table 2 Comparison of protein expression profiles in *R. rubrum* when PHB accumulation was stimulated by acetate addition

Protein name	UNIPROT	Pathway	Time point (h)		
			T24[a]	T30	T72
Ribulose bisphosphate carboxylase	Q2RRP5	Calvin cycle	62.7[b]	74.0	29.8
Pyruvate dehydrogenase (lipoamide)	Q2RT64	Pyruvate metabolism	1024	685	385
Pyruvate dehydrogenase beta subunit	Q2RT65		1030	684	486
Dihydrolipoamide acetyltransferase, long form	Q2RT66		932	625	409
Dihydrolipoyl dehydrogenase	Q2RT67		90	75	40
	Q2RV29		144	169	169
Acetyl-CoA hydrolase	Q2RT18		142	292	465
Succinate dehydrogenase	Q2RV42	TCA cycle	83	123	98
Phasin	Q2RP67	PHB metabolism	1270	1490	4860
	Q2RQI1		210	923	4500
Butyryl-CoA dehydrogenase	Q2RUT6		47.1	4.4	1.7
PhaR	Q2RXR4		96	72	171
Crotonyl-CoA reductase	Q2RPT7	Ethylmalonyl-CoA pathway	178	258	140
Methylmalonyl-CoA epimerase	Q2RU23		50.4	109	35.6
Methylmalonyl-CoA mutase	Q2RPT8		16.9	22.2	7.4

Proteins expressed with significant difference under tested conditions are presented. Protein relative abundance is expressed as summed ion intensities for a given protein, as calculated by the MaxQuant programme (Cox and Mann 2008; Cox et al. 2011)

[a] The T24 sample was taken before the acetate addition

[b] Label-free quantification (LFQ) values representing the average protein expression level of three biological replicates and two technical replicates. LFQ × 10^8 , e.g. 62.7 × 10^8

to encode 3850 proteins and 83 RNAs (Munk et al. 2011). Over 130,000 peptide tandem mass spectra were used to identify 11,495 unique peptides, in turn generating 1845 high-confidence (≥0.99 ProteinProphet score) protein identifications. This represents a substantial proportion (48 %) of the predicted *R. rubrum* proteome and reflects the extensive MS analysis. Moreover, the proteins exhibited a wide range of annotated biophysical (molecular mass, isoelectric point), biochemical (functional annotations) and structural (domains) properties, suggesting that the analysis was not biased in favour of, or against, any protein class. LFQ was used as a semi-quantitative measure of protein abundance, which allowed for monitoring the protein expression patterns in different samples (Cagney et al. 2005; Wang et al. 2003).

The changes in the *R. rubrum* proteome associated with acetate addition and stimulation of PHB accumulation were analysed (Table 2; Online Resource, Table S1). The proteins with different expression patterns (578 proteins; Table S1) over the growth period were mapped to different metabolic pathways (Table 2).

PHB synthesis stimulated by acetate addition affects the expression and activity of RuBisCO

Surprisingly, RuBisCO was detected in the proteome of *R. rubrum* grown aerobically in the dark (Table 2). RuBisCO is an enzyme involved in CO_2 fixation and to date is associated exclusively with anaerobic growth of *R. rubrum* S1 (Grammel et al. 2003). RuBisCO was detected at all time points analysed, with a 2.5-fold decrease observed between T30 and T72 (Table 2). The other enzymes of the Calvin cycle were also present, but there was no significant change in their relative expression across the cultivation period (Online Resource, Table S1). The expression of the RuBisCO large subunit did not show a statistically significant change over the growth period (Online Resource, Table S1). However, to determine whether the detected enzyme is active and whether there is a difference in the activity with regard to PHB accumulation, we measured the RuBisCO activity in cell-free extracts of *R. rubrum.* Cell-free extracts exhibited RuBisCO activity, which was highest at T24 and T25, and decreased over the cultivation period (Fig. 2). There was an 11-fold difference in RuBisCO activity between T24 and T72. PHB was first detected at T36 (about 3 % of CDW, Fig. 1a), which coincided with a 5-fold decrease in RuBisCO activity compared to T24 (Fig. 2). Malate-grown *R. rubrum* accumulated low levels of PHB (8 %, Online Resource, Fig. S3). These cells exhibited a 2.7-fold decrease in RuBisCO activity between T24 and T72 (Online Resource, Fig. S4).

The RuBisCO activity was also detected in *R. rubrum* Δ*pha*C1Δ*pha*C2 (Fig. 2). The activity remained at the same level over the course of the cultivation period, suggesting that

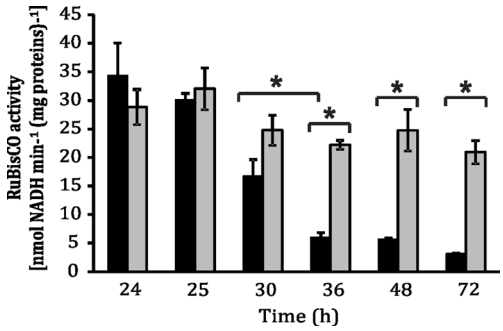

Fig. 2 RuBisCO activity was assayed by following the rate of NADH oxidation by cell-free extracts of *R. rubrum* (*black bars*) and *R. rubrum* Δ*phaC1*Δ*phaC2* (*grey bars*) using ribulose 1,5-biphosphate as the substrate. The *asterisks* represent statistically significant difference between the wild-type and mutant strains and different time points. The *error bars* represent standard deviation between three biological replicates

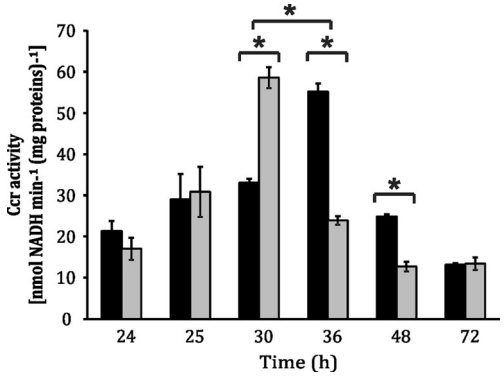

Fig. 3 Comparison of Ccr activity exhibited by cell-free extracts of *R. rubrum* (*black bars*) and *R. rubrum* Δ*phaC1*Δ*phaC2* (*grey bars*) grown aerobically in the dark with malate and acetate as cosubstrates. The Ccr activity is expressed as the rate of NADH oxidation. The *asterisks* represent statistically significant difference ($p < 0.05$) in Ccr activity between the wild-type and mutant strains and different time points. The *error bars* represent standard deviation between three biological replicates

the decrease in RuBisCO activity in the wild-type strain was associated with PHB accumulation.

The expression of core proteins of the ethylmalonyl-CoA pathway is affected by acetate

Signature proteins of the EMC pathway, previously described as a new acetate assimilation strategy in a purple non-sulphur bacterium *R. sphaeroides* (Erb et al. 2009b), were identified in the proteome of *R. rubrum* grown aerobically in the dark (Table 2). The EMC pathway and PHB synthesis pathway share the first two steps i.e. condensation of two acetyl-CoA molecules into acetoacetyl-CoA which is subsequently reduced to (*R*)-3-hydroxybutyryl-CoA (Alber et al. 2006). (*R*)-3-hydroxybutyryl-CoA is further reduced to crotonyl-CoA in the EMC pathway or polymerised to PHB. Therefore, these two synthetic pathways compete for the same intermediate. The signature enzymes of the EMC pathway, Ccr, methylmalonyl-CoA epimerase and methyl-malonyl-CoA mutase showed a 1.3- to 2.2-fold increase in relative expression levels in MA-grown cells between T24 and T30, suggesting that acetate was assimilated via the EMC pathway (Alber et al. 2006; Erb et al. 2009b). Indeed, cells grown on malate alone had up to 2-fold lower levels of EMC pathway core proteins at T30 compared to MA-grown cells (Online Resource, Table S1). The expression of the EMC pathway core proteins decreased between T30 and T72, after cells started to accumulate PHB (Table 2). An established enzymatic assay was used to confirm the presence of Ccr and to establish if accumulation of PHB affects its activity (Erb et al. 2009a). Erb and colleagues proposed that Ccr requires NADPH as a cofactor, crotonyl-CoA as a substrate and CO_2 for the activity (Erb et al. 2007; Erb et al. 2009a). While no reaction occurred when NADPH was used as the cofactor, NADH oxidation by the cell-free extracts of *R. rubrum* was observed (Fig. 3). Appropriate controls showed that the cell extract did not oxidise NADH in the absence of crotonyl-CoA. The enzyme was able to catalyse the reaction in the absence of CO_2. However, the reaction was about 3-fold higher in the presence of CO_2 suggesting that the enzyme is more active at carboxylating crotonyl-CoA than simply reducing it. The Ccr activity increased 1.8-fold 1 h after acetate addition (Fig. 3), with the highest activity achieved at T36. PHB accumulation was detected at T36, and a 5-fold increase in PHB levels between T36 and T48 was accompanied by a 2-fold decrease in Ccr activity (Fig. 3). The Ccr activity was detected in *R. rubrum* grown with malate only (Online Resource, Fig. S5). However, MA-grown cells exhibited 1.8-fold higher activity compared to malate-grown cells at T30 and T36 (Online Resource, Fig. S5).

The peak of Ccr activity in *R. rubrum* Δ*pha*C1Δ*pha*C2 was detected at an earlier time point in comparison with that in the wild type (Fig. 3). It seems that when PHB accumulation is allowed, the common precursor (*R*)-3-hydroxybutyryl-CoA is first directed to PHB synthesis, which may stimulate the activity of the EMC pathway and acetate assimilation into biomass. At T48, the Ccr activity decreases in both the wild-type and the PHB-negative strains (Fig. 3). However, the activity is 2-fold higher in the wild type possibly allowing more acetate to be assimilated into biomass.

The effect of acetate addition on enzymes involved in central metabolic pathways and PHB metabolism

The enzymes of the PDC, pyruvate dehydrogenase (subunits α and β), dihydrolipoyl transacetylase and dihydrolipoyl dehydrogenase showed differences in their relative expression levels in *R. rubrum* after acetate was added to the growth medium (Table 2). The PDC is a large membrane-bound complex in *R. rubrum* and serves as the main gateway into the TCA cycle during aerobic metabolism (Berg et al. 2002; Lüderitz and Klemme 1977). The PDC oxidatively

decarboxylates pyruvate to form the activated acetate i.e. acetyl-CoA, a high-energy intermediate that sits at the crossroads of central metabolism (Bentley 2000; Kennedy 2001). Six hours after acetate addition, a 1.2–1.5-fold decrease in relative expression levels of all PDC enzymes was observed, possibly as an effect of acetyl-CoA formation. According to the KEGG database (1), two enzymes can also be involved in acetate activation: acetyl-CoA synthase (Q2RNC6) and acetyl-CoA hydrolase (Q2RT18). While both enzymes were detected under both conditions, the hydrolase showed a 2-fold increase in relative expression levels 6 h after acetate addition (T30) and a 3.3-fold increase at T72 (Table 2).

Despite the fact that no PHB was detected at T24 and there was an 8-fold increase in PHB levels between T36 and T72 (Fig. 1a), the majority of proteins involved in PHB metabolism did not show a significant difference over the cultivation period (Online Resource, Table S1). However, the phasin Q2RP67, a protein covering the surface of PHB storage granules, had a 3.8-fold higher expression at T72 compared to T24 (Table 1). An increase in expression was observed for phasin Q2RQI1, with a 4.4-fold increase at T30 and a 21.4-fold increase in relative expression levels at T72 compared to T24. The expression of PhaR (Q2RXR4), another granule-bound protein, was observed at all time points tested and increased 2.3-fold between T30 and T72.

High expression levels of the synthase PhaC2 (Q2RRN2), which catalyses the polymerisation of (*R*)-3-hydroxybutyryl-CoA, were observed at T24 and T30, before any PHB was detected (Online Resource, Table S1; Fig. 1). Similar to the PhaC2 (Q2RRN2), the expression of PHB depolymerases Q2RNZ5 and Q2RU10 was detected at T24 and remained at the same level throughout the cultivation period (Online Resource, Table S1). Early expression (T24) of PHB metabolism-related proteins and simultaneous expression of the polymerase and depolymerases reflect a highly dynamic nature of PHB metabolism and its involvement in processes other than simple carbon and energy storage.

The differences in proteome are reflected in metabolite levels in *R. rubrum* S1

(*R*)-3-hydroxybutyrate, a monomer unit of PHB, was detected as an intracellular metabolite (Table 3). Since PHB synthesis and degradation occur simultaneously in bacterial cells, the detected (*R*)-3-hydroxybutyrate could be the precursor for PHB synthesis as well as the degradation product of PhaZ activity (Uchino et al. 2007). Succinate was amongst the most abundant metabolites detected in cell extracts of *R. rubrum* grown aerobically in the dark. Succinate levels first increased 3.1-fold, followed by a 1.7-fold decrease (Table 3). This is in keeping with the expression and activity of the EMC pathway signature enzyme (Fig. 3), with succinyl-CoA being one of the products of this pathway. The presence of intracellular acetate at T24, before acetate addition (Table 3), suggests malate is metabolised to acetate in *R. rubrum*. Acetate was detected in *R. rubrum* grown with malate as a sole source of carbon and energy as well (Online Resource, Table S2). A 2.7-fold increase of acetate levels at T36 is probably the combined effect of acetate addition to malate-grown cells at T24 and the ability of M-grown cells to produce acetate from malate (Table 3).

Glutamate is a nitrogen donor in many biosynthetic reactions, and it was previously shown that this amino acid was the dominant amino acid in cell extracts of *R. rubrum* grown both under nitrogenase repressed and derepressed conditions (Kanemoto and Ludden 1987). Nitrogen limitation occurred at T48 of the cultivation period (Fig. 1). Unlike in the case reported by Kanemoto and Ludden, where the glutamate level decreased under nitrogen limitation, in our experiments intracellular glutamate increased at T72 compared to T36 (Table 3).

Table 3 Metabolite levels in *R. rubrum* when PHB accumulation was stimulated by acetate addition at T24 to malate grown cells

Metabolites[a]	Time point (h)						
	T24		T36		T72		*P* value
	Mean	SD	Mean	SD	Mean	SD	
3-Hydroxybutyrate	1.2a[a]	0.6	4.7b	0.8	10.7c	3.8	<0.001
Acetate	8.8a	4.3	24.0b	3.0	15.5c	5.2	<0.001
Glutamate	25.9ab	9.2	20.4a	2.9	31.1b	6.1	0.007
Succinate	5.5a	2.4	17.1b	2.2	10.2c	2.1	<0.001
Butyrate	2.1a	1.0	16.4b	2.6	8.4c	1.6	<0.001
Lactate	3.2a	1.4	3.7a	1.0	6.7b	2.1	<0.000
Propionate	1.3a	0.7	3.8b	0.9	4.5b	0.5	<0.001
Fumarate	0.5a	0.2	0.2b	0.07	0.4ab	0.2	0.029
Malate	51.6a	14.3	9.6b	3.6	12.6b	3.6	<0.001

All values are obtained as average of 10 biological replicates. Different lowercase letters indicate significant difference between the analysed time points (T24, T36, T72)

[a] Metabolites are represented as a percentage of the abundant metabolites

Discussion

Redox homeostasis is a fundamental requirement for sustained metabolism and growth in all biological systems. The intracellular redox potential is determined by the NADH/NAD$^+$ and the NADPH/NADP$^+$ ratio (Green and Paget 2004). Principally, high intracellular energy charge, characterised by an elevated pool of acetyl-CoA, NAD(P)H, ATP and others, promotes PHA formation (Haywood et al. 1988; Uchino et al. 2007). The levels of ATP and NADPH increased in *R. rubrum* after acetate was added (Online

Resource, Fig. S2), which can explain the onset of PHB accumulation (Fig. 1). In addition, NAD(P)H and acetyl-CoA negatively regulate the activity of the enzymes of the PDC (Lüderitz and Klemme 1977). Indeed, after acetate addition to the malate-grown *R. rubrum*, the expression of PDC enzymes decreased (Table 2) which led to a decrease in malate consumption (Fig. 1b).

What is surprising is that acetate assimilation into biomass is stimulated by the presence of PHB since the PHB-negative mutant consumes 2-fold less acetate and that acetate assimilation into biomass is much more efficient than into PHB under PHB-accumulating conditions (Table 1). It is widely reported that PHB can function as a carbon and energy storage material (Grage et al. 2009; Steinbüchel and Lütke-Eversloh 2003; Verlinden et al. 2007), forms complexes with calcium and polyphosphate for DNA uptake (Madison and Huisman 1999) and is involved in stress response (Pham et al. 2004; Raberg et al. 2014). It was also suggested that PHA might be involved in maintenance of efficient metabolism (Escapa et al. 2012). The early and simultaneous expression of the proteins involved in the PHB metabolism (Table 2; Online Resource, Table S1) suggests that the PHB synthesis and degradation operate as a continuous cycle, potentially optimising the carbon flow in the organism. Furthermore, PHB is likely acting as an electron sink in *R. rubrum* as well as a carbon storage material. *R. rubrum* uses hydrogen as an electron sink and the Calvin cycle to distribute excess electrons in the cell (Gordon and McKinlay 2014). When grown aerobically in the dark, *R. rubrum* cannot produce hydrogen (Ormerod et al. 1961; Selao et al. 2011). Furthermore, RuBisCO has not been reported to be expressed or active in aerobically grown *R. rubrum* (Cook et al. 1988; Grammel et al. 2003). Thus, the organism when grown aerobically in the dark would lack two key means to metabolise excess electrons. However, we observed that the expression of active RuBisCO in *R. rubrum* grown aerobically and the presence of PHB coincide with the reduction of RuBisCO activity. The decarboxylation of malate to pyruvate and pyruvate to acetyl-CoA (Kleijn et al. 2010) could stimulate RuBisCO expression. Indeed, we observed the presence of pyruvate dehydrogenase and malate decarboxylase (malic enzyme) in the proteome of *R. rubrum* (Table 2; Online Resource, Table S1). Furthermore, acetate was detected as one of the metabolites in *R. rubrum* when only malate was supplied as a carbon and energy source (T24; Table 3), suggesting malate is metabolised to acetyl-CoA through oxidative decarboxylation.

The normal role of RuBisCO and the Calvin cycle would be to metabolise carbon dioxide and oxidise reduced cofactors such as NAD(P)H (Gordon and McKinlay 2014). When this is coupled to metabolic pathways that reduce these cofactors, such as oxidative decarboxylation of malate (Kleijn et al. 2010), the cell has a closed cycle of electron flow (Fig. 4). However, PHB synthesis also requires reduced cofactors such as NAD(P)H. Thus, it is logical that RuBisCO expression and

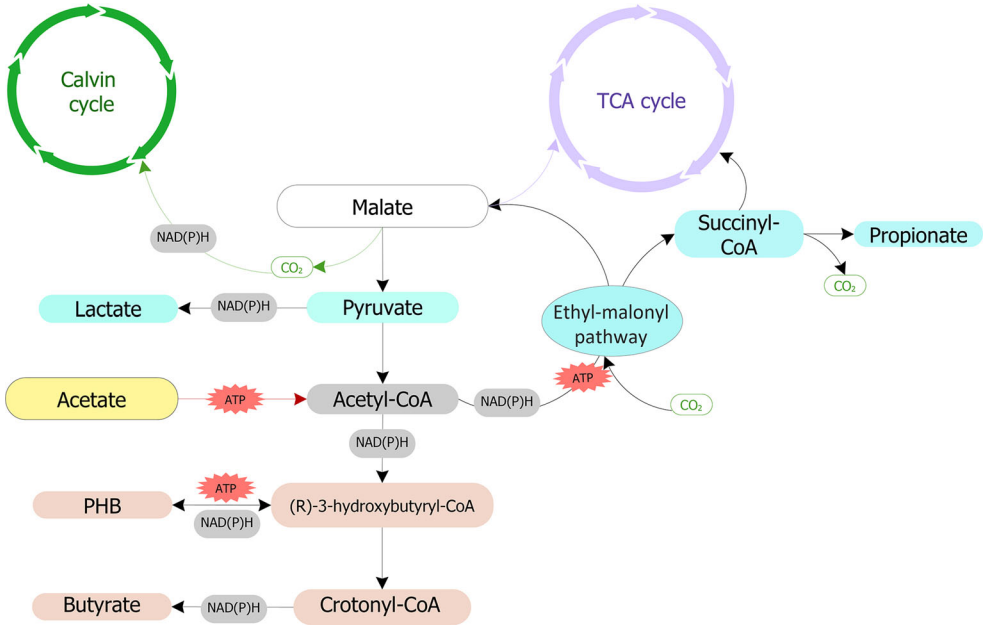

Fig. 4 The metabolism of malate and acetate in *R. rubrum* during aerobic growth in the dark. The main metabolic pathways with differential expression of enzymes involved and the intracellular metabolites that showed significant difference under tested growth conditions are depicted. Distinct pathways are represented by *different colours*. Intracellular metabolites with a significant change upon acetate addition are depicted in *different colours* to mark potential pathways where these metabolites could arise. The interchangeable forms of NAD(P)H suggest that reducing equivalents formed in a catabolic process could be recycled in an anabolic process, and vice versa. *R. rubrum* possesses an H^+-translocating transhydrogenase (Table S1; Q2RSB2, Q2RSB4), which couples the transfer of hydride-ion equivalents between NAD(H) and NADP(H)

activity decrease with PHB accumulation to prevent oxidation of the reduced cofactors by the Calvin cycle and allow their oxidation for PHB precursor synthesis (Figs. 1, 2, and 4 and Table 1). Under photoautotrophic conditions, the level of CO_2 and the presence of reaction by-products regulate the level of RuBisCO expression and activity (Leustek et al. 1988; Pearce 2006). While end product repression by acetyl-CoA and related metabolites was observed in *P. oxalaticus* (Meijer and Dijkhuizen 1988), the addition of acetate did not repress RuBisCO activity in *R. rubrum*, as RuBisCO activity under aerobic, dark conditions in the PHB-negative mutant remains constant over time (Fig. 2). Thus, the decrease in expression and activity of RuBisCO is a consequence of stimulated PHB accumulation (Figs. 1 and 2). It is possible that PHB takes over the role of the main electron sink in *R. rubrum*, thereby maintaining the redox homeostasis.

R. rubrum lacks isocitrate lyase, hence the glyoxylate shunt is not operative (Kornberg and Lascelles 1960). Acetate is most likely assimilated through the EMC pathway (Alber et al. 2006), as we detected the expression of signature enzymes of this pathway (Table 1). The presence of acetate coincides with changes in PHB levels and both the activity and expression of the first enzyme of the core part of the EMC pathway namely Ccr (Fig. 3). The higher expression of the core proteins at T30 (Table 2) is likely a result of the presence of acetate. There was a difference in the peak of Ccr activity between the wild-type and the PHB-negative mutant (Fig. 3). When PHB accumulation was allowed, the Ccr activity was highest at T36, while the highest activity in the PHB-negative mutant occurred at T30. It is possible that under PHB-accumulating conditions, (*R*)-3-hydroxybutyric acid, the common intermediate for the PHB and EMC pathways, was firstly polymerised into PHB, as evidenced from the later increase in Ccr activity in the wild-type strain. However, the increase in Ccr activity was followed by a decrease in both the wild type and the mutant (Fig. 3). The decrease in expression levels of the core proteins of the EMC pathway at T72 is unlikely to be a response to higher levels of PHB as the mutant strain has a similar profile of Ccr activity (Fig. 4). A 2.3-fold increase in the common intermediate of the EMC pathway and PHB synthesis of (*R*)-3-hydroxybutyric acid was detected in *R. rubrum* between T36 and T72 (Table 3). This might be the consequence of the decreased Ccr activity. As there was no further increase in PHB level after 72 h of cultivation (data not shown) and PHB synthesis and degradation occur simultaneously in bacterial cells, the increase in (*R*)-3-hydroxybutyrate could also be the consequence of the PhaZ activity (Uchino et al. 2007).

Another finding supporting the active EMC pathway in *R. rubrum* is the presence of succinate as an intracellular metabolite (Table 3) (Erb et al. 2007). The difference in expression levels of enzymes belonging to the EMC pathway at T24 and T30 corresponded with the 3.1-fold difference in succinate between T24 and T36 (Tables 1 and 2). Succinate was not detected as a metabolite during aerobic growth of *R. rubrum* in the dark in defined mineral medium used by Rudolf and Grammel (2012), indicating increased flux through the EMC pathway.

Fig. 4 summarises results and shows the connection between MA metabolism, PHB metabolism, the EMC pathway and the Calvin cycle. During aerobic growth of *R. rubrum* with malate as a carbon and energy source, malate is oxidatively decarboxylated to pyruvate, and pyruvate is further decarboxylated to acetyl-CoA, generating CO_2 and NAD(P)H which could fuel the Calvin cycle (Fig. 4). In addition, produced CO_2 allows acetate assimilation (Eisenberg 1953), and assimilated acetate acts as a direct precursor for PHB synthesis (Fig. 4). When PHB accumulation is stimulated in *R. rubrum* by acetate addition, it further stimulates the conversion of acetate into biomass, thus driving carbon flow in a direction contrary to the normal perceived flow. Furthermore, PHB becomes the main electron sink in the cell, decreasing the role of the Calvin cycle but not affecting the EMC pathway (Gordon and McKinlay 2014; Laguna et al. 2011).

Compliance with ethical standards This article does not contain any studies with human participants or animals performed by any of the authors.

Funding information This work was funded by the European Commission's The Seventh Framework Programme project SYNPOL (311815).

Conflict of interest The authors declare that they have no conflict of interest.

References

(2015) KEGG. Publisher. http://www.genome.jp/dbget-bin/www_bfind?T00310

Alber BE, Spanheimer R, Ebenau-Jehle C, Fuchs G (2006) Study of an alternate glyoxylate cycle for acetate assimilation by *Rhodobacter sphaeroides*. Mol Microbiol 61(2):297–309. doi:10.1111/J.1365-2958.2006.05238.X

Arias S, Bassas-Galia M, Molinari G, Timmis KN (2013) Tight coupling of polymerization and depolymerization of polyhydroxyalkanoates ensures efficient management of carbon resources in *Pseudomonas putida*. Microb Biotechnol 6(5):551–563. doi:10.1111/1751-7915.12040

Basak N, Das D (2007) The prospect of purple non-sulfur (PNS) photosynthetic bacteria for hydrogen production: the present state of the art. World J Microbiol Biotechnol 23(1):31–42. doi:10.1007/s11274-006-9190-9

Bentley R (2000) From 'reactive C-2 units' to acetyl coenzyme A: a long trail with an acetyl phosphate detour. Trends Biochem Sci 25(6): 302–305. doi:10.1016/S0968-0004(00)01590-5

Berg JM, Tymoczko JL, Stryer L (2002) Biochemistry, Fifth edn. W. H. Freeman and Company, New York

Bose SK, Gest H, Ormerod JG (1961) Light-activated hydrogenase activity in a photosynthetic bacterium—a permeability phenomenon. J Biol Chem 236(3):PC13–PC14

Brandl H, Knee EJ, Fuller RC, Gross RA, Lenz RW (1989) Ability of the phototrophic bacterium *Rhodospirillum rubrum* to produce various poly (beta-hydroxyalkanoates)—potential sources for biodegradable polyesters. Int J Biol Macromol 11(1):49–55. doi:10.1016/0141-8130(89)90040-8

Cagney G, Park S, Chung C, Tong B, O'Dushlaine C, Shields DC, Emili A (2005) Human tissue profiling with multidimensional protein identification technology. J Proteome Res 4(5):1757–1767. doi:10.1021/Pr0500354

Carius AB, Henkel M, Grammel H (2011) A glutathione redox effect on photosynthetic membrane expression in *Rhodospirillum rubrum*. J Bacteriol 193(8):1893–1900. doi:10.1128/JB.01353-10

Carius L, Carius AB, McIntosh M, Grammel H (2013) Quorum sensing influences growth and photosynthetic membrane production in high-cell-density cultivations of *Rhodospirillum rubrum*. BMC Microbiol 13. doi:10.1186/1471-2180-13-189

Cook LS, Im H, Tabita FR (1988) Oxygen-dependent inactivation of ribulose 1,5-bisphosphate carboxylase oxygenase in crude extracts of *Rhodospirillum rubrum* and establishment of a model inactivation system with purified enzyme. J Bacteriol 170(12):5473–5478

Cox J, Mann M (2008) MaxQuant enables high peptide identification rates, individualized p.p.b.-range mass accuracies and proteome-wide protein quantification. Nat Biotechnol 26(12):1367–1372. doi:10.1038/nbt.1511

Cox J, Neuhauser N, Michalski A, Scheltema RA, Olsen JV, Mann M (2011) Andromeda: a peptide search engine integrated into the MaxQuant environment. J Proteome Res 10(4):1794–1805. doi:10.1021/Pr101065j

Do YS, Smeenk J, Broer KM, Kisting CJ, Brown R, Heindel TJ, Bobik TA, DiSpirito AA (2007) Growth of *Rhodospirillum rubrum* on synthesis gas: conversion of CO to H_2 and poly-beta-hydroxyalkanoate. Biotechnol Bioeng 97(2):279–286. doi:10.1002/bit.21226

Eggers J, Steinbüchel A (2014) Impact of *Ralstonia eutropha*'s poly(3-hydroxybutyrate) (PHB) depolymerases and phasins on PHB storage in recombinant *Escherichia coli*. Appl Environ Microbiol 80(24):7702–7709. doi:10.1128/Aem.02666-14

Eisenberg MA (1953) The tricarboxylic acid in *Rhodospirillum rubrum*. J Biol Chem 203(2):815–836

Erb TJ, Berg IA, Brecht V, Müller M, Fuchs G, Alber BE (2007) Synthesis of C5-dicarboxylic acids from C2-units involving crotonyl-CoA carboxylase/reductase: the ethylmalonyl-CoA pathway. Proc Natl Acad Sci U S A 104(25):10631–10636. doi:10.1073/pnas.0702791104

Erb TJ, Brecht V, Fuchs G, Müller M, Alber BE (2009a) Carboxylation mechanism and stereochemistry of crotonyl-CoA carboxylase/reductase, a carboxylating enoyl-thioester reductase. Proc Natl Acad Sci U S A 106(22):8871–8876. doi:10.1073/pnas.0903939106

Erb TJ, Fuchs G, Alber BE (2009b) (2*S*)-Methylsuccinyl-CoA dehydrogenase closes the ethylmalonyl-CoA pathway for acetyl-CoA assimilation. Mol Microbiol 73(6):992–1008. doi:10.1111/j.1365-2958.2009.06837.x

Escapa IF, Garcia JL, Buhler B, Blank LM, Prieto MA (2012) The polyhydroxyalkanoate metabolism controls carbon and energy spillage in *Pseudomonas putida*. Environ Microbiol 14(4):1049–1063. doi:10.1111/j.1462-2920.2011.02684.x

Gordon GC, McKinlay JB (2014) Calvin cycle mutants of photoheterotrophic purple nonsulfur bacteria fail to grow due to an electron imbalance rather than toxic metabolite accumulation. J Bacteriol 196(6):1231–1237. doi:10.1128/JB.01299-13

Grage K, Peters V, Palamisany R, Rehm BH (2009) Polyhydroxyalkanoates: from bacterial storage compound via renewable plastic bio-bead. In: Rehm BH (ed) Microbial production of polymers and polymer precursors: applications and perspectives. Causter Academic Press, Norfolk, UK, pp. 255–289

Grammel H, Gilles ED, Ghosh R (2003) Microaerophilic cooperation of reductive and oxidative pathways allows maximal photosynthetic membrane biosynthesis in *Rhodospirillum rubrum*. Appl Environ Microbiol 69(11):6577–6586. doi:10.1128/Aem.69.11.6577-6586.2003

Green J, Paget MS (2004) Bacterial redox sensors. Nat Rev Microbiol 2(12):954–966. doi:10.1038/Nrmicro1022

Hauf W, Schlebusch M, Hüge J, Kopka J, Hagemann M, Forchhammer K (2013) Metabolic changes in *Synechocystis* PCC6803 upon nitrogen starvation: excess NADPH sustains polyhydroxybutyrate accumulation. Metabolites 3(1):101–118. doi:10.3390/metabo3010101

Haywood GW, Anderson AJ, Chu L, Dawes EA (1988) The role of NADH-linked and NADPH-linked acetoacetyl-CoA reductases in the poly-3-hydroxybutyrate synthesizing organism *Alcaligenes eutrophus*. FEMS Microbiol Lett 52(3):259–264. doi:10.1111/J.1574-6968.1988.Tb02607.X

Huang Da W, Sherman BT, Lempicki RA (2009) Bioinformatics enrichment tools: paths toward the comprehensive functional analysis of large gene lists. Nucleic Acids Res 37(1):1–13. doi:10.1093/nar/gkn923

Imhoff JF, Trüper HG (1992) The genus *Rhodospirillum* and related genera. In: Balows A, Trüper HG, Dworkin M, Harder W, Schleifer K-H (eds) Prokaryotes, 2nd edn. Berlin, Heidelberg, New York, Springer., pp. 2141–2155

Jendrossek D, Pfeiffer D (2014) New insights in the formation of polyhydroxyalkanoate granules (carbonosomes) and novel functions of poly(3-hydroxybutyrate). Environ Microbiol 16(8):2357–2373. doi:10.1111/1462-2920.12356

Kanemoto RH, Ludden PW (1987) Amino acid concentrations in *Rhodospirillum rubrum* during expression and switch-off of nitrogenase activity. J Bacteriol 169(7):3035–3043

Kennedy EP (2001) Hitler's gift and the era of biosynthesis. J Biol Chem 276(46):42619–42631. doi:10.1074/Jbc.R100051200

Klask C, Raberg M, Heinrich D, Steinbüchel A (2015) Heterologous expression of various PHA synthase genes in *Rhodospirillum rubrum*. Chem Biochem Eng Q 29(2):75–85

Kleijn RJ, Buescher JM, Le Chat L, Jules M, Aymerich S, Sauer U (2010) Metabolic fluxes during strong carbon catabolite repression by malate in *Bacillus subtilis*. J Biol Chem 285(3):1587–1596. doi:10.1074/Jbc.M109.061747

Koller M, Bona R, Hermann C, Horvat P, Martinz J, Neto J, Pereira L, Varila P, Braunegg G (2005) Biotechnological production of poly(3-hydroxybutyrate) with *Wautersia eutropha* by application of green grass juice and silage juice as additional complex substrates. Biocatal Biotransfor 23(5):329–337. doi:10.1080/10242420500292252

Kornberg HL, Lascelles J (1960) The formation of isocitratase by the *Athiorhodaceae*. J Gen Microbiol 23(3):511–517

Lageveen RG, Huisman GW, Preusting H, Ketelaar P, Eggink G, Witholt B (1988) Formation of polyesters by *Pseudomonas oleovorans*: effect of substrates on formation and composition of poly-(R)-3-hydroxyalkanoates and poly-(R)-3-hydroxyalkenoates. Appl Environ Microbiol 54(12):2924–2932

Laguna R, Tabita FR, Alber BE (2011) Acetate-dependent photoheterotrophic growth and the differential requirement for the Calvin-Benson-Bassham reductive pentose phosphate cycle in *Rhodobacter sphaeroides* and *Rhodopseudomonas palustris*. Arch Microbiol 193(2):151–154. doi:10.1007/S00203-010-0652-Y

Leustek T, Hartwig R, Weissbach H, Brot N (1988) Regulation of ribulose bisphosphate carboxylase expression in *Rhodospirillum rubrum*: characteristics of messenger RNA synthesized *in vivo* and *in vitro*. J Bacteriol 170(9):4065–4071

Lüderitz R, Klemme JH (1977) Isolation and characterization of a membrane-bound pyruvate-dehydrogenase complex from

phototropic bacterium *Rhodospirillum rubrum*. Z Naturforsch C J Biosci 32(5–6):351–361

Madison LL, Huisman GW (1999) Metabolic engineering of poly(3-hydroxyalkanoates): from DNA to plastic. Microbiol Mol Biol R 63(1):21−+

Meijer WG, Dijkhuizen L (1988) Regulation of autotrophic metabolism in *Pseudomonas oxalaticus* OX1 wild-type and an isocitrate-lyase-deficient mutant. J Gen Microbiol 134:3231–3237

Munk AC, Copeland A, Lucas S, Lapidus A, Del Rio TG, Barry K, Detter JC, Hammon N, Israni S, Pitluck S, Brettin T, Bruce D, Han C, Tapia R, Gilna P, Schmutz J, Larimer F, Land M, Kyrpides NC, Mavromatis K, Richardson P, Rohde M, Goker M, Klenk HP, Zhang YP, Roberts GP, Reslewic S, Schwartz DC (2011) Complete genome sequence of *Rhodospirillum rubrum* type strain (S1(T)). Stand Genomic Sci 4(3):293–302. doi:10.4056/Sigs.1804360

Ormerod JG, Gest H, Ormerod KS (1961) Light-dependent utilization of organic compounds and photoproduction of molecular hydrogen by photosynthetic bacteria—relationships with nitrogen metabolism. Arch Biochem Biophys 94(3):449-&. doi:10.1016/0003-9861(61)90073-X

Pearce FG (2006) Catalytic by-product formation and ligand binding by ribulose bisphosphate carboxylases from different phylogenies. Biochem J 399:525–534. doi:10.1042/Bj20060430

Pham TH, Webb JS, Rehm BH (2004) The role of polyhydroxyalkanoate biosynthesis by *Pseudomonas aeruginosa* in rhamnolipid and alginate production as well as stress tolerance and biofilm formation. Microbiol SGM 150(Pt 10):3405–3413. doi:10.1099/mic.0.27357-0

Raberg M, Voigt B, Hecker M, Steinbüchel A (2014) A closer look on the polyhydroxybutyrate- (PHB-) negative phenotype of *Ralstonia eutropha* PHB(−)4. Plos One 9(5) ARTN e95907. doi:10.1371/journal.pone.0095907

Reid CD, Tissue DT, Fiscus EL, Strain BR (1997) Comparison of spectrophotometric and radioisotopic methods for the assay of Rubisco in ozone-treated plants. Physiol Plant 101(2):398–404. doi:10.1111/j.1399-3054.1997.tb01014.x

Rudolf C, Grammel H (2012) Fructose metabolism of the purple non-sulfur bacterium *Rhodospirillum rubrum*: effect of carbon dioxide on growth, and production of bacteriochlorophyll and organic acids. Enzym Microb Technol 50(4–5):238–246. doi:10.1016/j.enzmictec.2012.01.007

Scheiner D (1976) Determination of ammonia and Kjeldahl nitrogen by indophenol method. Water Res 10(1):31–36. doi:10.1016/0043-1354(76)90154-8

Selao TT, Edgren T, Wang H, Noren A, Nordlund S (2011) Effect of pyruvate on the metabolic regulation of nitrogenase activity in *Rhodospirillum rubrum* in darkness. Microbiol SGM 157:1834–1840. doi:10.1099/Mic.0.045831-0

Smith RL, West TP, Gibbons WR (2008) *Rhodospirillum rubrum*: utilization of condensed corn solubles for poly-(3-hydroxybutyrate-co-3-hydroxyvalerate) production. J Appl Microbiol 104(5):1488–1494. doi:10.1111/j.1365-2672.2007.03685.x

Steinbüchel A, Lütke-Eversloh T (2003) Metabolic engineering and pathway construction for biotechnological production of relevant polyhydroxyalkanoates in microorganisms. Biochem Eng J 16(2):81–96. doi:10.1016/S1369-703x(03)00036-6

Uchino K, Saito T, Gebauer B, Jendrossek D (2007) Isolated poly(3-hydroxybutyrate) (PHB) granules are complex bacterial organelles catalyzing formation of PHB from acetyl coenzyme A (CoA) and degradation of PHB to acetyl-CoA. J Bacteriol 189(22):8250–8256. doi:10.1128/Jb.00752-07

Verlinden RAJ, Hill DJ, Kenward MA, Williams CD, Radecka I (2007) Bacterial synthesis of biodegradable polyhydroxyalkanoates. J Appl Microbiol 102(6):1437–1449. doi:10.1111/j.1365-2672.2007.03335.x

Wang WX, Zhou HH, Lin H, Roy S, Shaler TA, Hill LR, Norton S, Kumar P, Anderle M, Becker CH (2003) Quantification of proteins and metabolites by mass spectrometry without isotopic labeling or spiked standards. Anal Chem 75(18):4818–4826. doi:10.1021/Ac026468x

Zhao YH, Li HM, Qin LF, Wang HH, Chen GQ (2007) Disruption of the polyhydroxyalkanoate synthase gene in *Aeromonas hydrophila* reduces its survival ability under stress conditions. FEMS Microbiol Lett 276(1):34–41. doi:10.1111/j.1574-6968.2007.00904.x